CRYSTAL GROWTH & DESIGN

pubs.acs.org/crystal

Article

Exploring Coral Calcification by Calcium Carbonate Overgrowth Experiments

Tal Zaquin, Iddo Pinkas, Anna Paola Di Bisceglie, Angelica Mucaria, Silvia Milita, Simona Fermani, Stefano Goffredo, Tali Mass,* and Giuseppe Falini*

Cite This: *Cryst. Growth Des.* 2022, 22, 5045−5053

Read Online

ACCESS | Metrics & More | Article Recommendations | Supporting Information

ABSTRACT: The Scleractinia coral biomineralization process is a representative example of a heterogeneous process of nucleation and growth of biogenic $CaCO_3$ over a mineral phase. Indeed, even if the biomineralization process starts before settlement, the bulk formation of the skeleton takes place only when the larvae attach to a solid substrate, which can be Mg-calcite from coralline algae, and the following growth proceeds on the Mg-calcite surface of the formed baseplate of the planula. Despite this peculiarity and central role of the Mg-calcite substrate, the *in vitro* overgrowth of $CaCO_3$ on single crystals of Mg-calcite, or calcite, in the presence of magnesium ions and the soluble organic matrix (SOM) extracted from coral skeletons has not been performed until now. In this study, the SOMs from *Stylophora pistillata* and *Oculina patagonica* skeletons were used in a set of overgrowth experiments. The overgrown $CaCO_3$ was characterized by microscopic, diffractometric, and spectroscopic techniques. Our results showed that $CaCO_3$ overgrowth in the presence of *S. pistillata* or *O. patagonica* SOM produces different effects. However, there appears to be a minor distinction between samples when magnesium ions are present in solution. Moreover, the Mg-calcite substrate appears to be a favorable substrate for the overgrowth of aragonite, differently from calcite. These observations fit with the observed settling of coral larvae on Mg-calcite-based substrates and with the *in vivo* observation that in the planula aragonite forms on first-formed Mg-calcite crystals. The overall results of this study highlight the importance of magnesium ions, either in the solution or in the substrate, in defining the shape, morphology, and polymorphism of biodeposited $CaCO_3$. They also suggest a magnesium-dependent biological control on the deposition of coral skeletons.

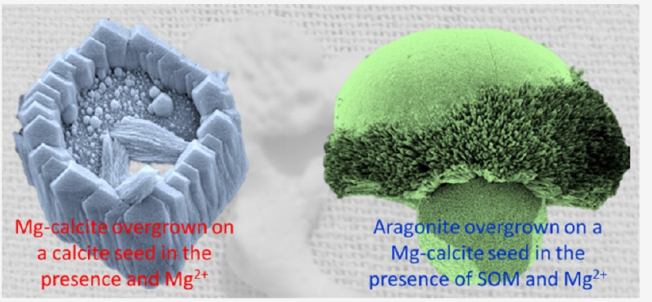

INTRODUCTION

In living systems, minerals are almost ubiquitous components of bacteria, plants, fungi, and animals of all types in which they serve a multitude of crucial structural and biochemical functions.[1−3] Biominerals, minerals of biogenic origin, form at moderate ambient temperatures and pressures in conditions of high concentrations of the mineralizing ions, using catalytic aids, and crystallize in unique patterns related to the biological and ecological environment in which they are biosynthesized.[1,2,4,5]

The mechanisms by which organisms form mineralized skeletons have been a major research focus. Among the most relevant discoveries is the observation that different organisms use a similar mechanism to form biomineralized structures based on an amorphous precursor.[6,7] Accordingly, the formation of these mineralized structures occurs by particle attachment on a mineral and/or biological matrix.[8] As a consequence, in many cases, the formation of calcium carbonate ($CaCO_3$) biomineralized structures as diverse as coral skeletons,[9,10] molluscan shells,[11] and sea urchin spines[12] occurs *via* a heterogeneous growth process through a transient amorphous phase. This mechanism involves intraskeletal organic molecules, mainly by their soluble fraction usually referred to as the soluble organic matrix (SOM), and specific ions, among which magnesium plays a key role. The relevance of magnesium ions in $CaCO_3$ precipitation processes has been highlighted in different aspects. It has been demonstrated that the magnesium/calcium molar ratio in solution controls the polymorphic selection with the formation of Mg-calcite, aragonite,[13] monohydrocalcite,[14] and amorphous calcium carbonate (ACC),[15] among the most relevant phases. In the context of $CaCO_3$ biomineralization, the stabilization of ACC by magnesium ions has been intensely discussed,[16] where the potential roles of magnesium ions in controlling the mineralizing activity of SOM molecules have been suggested.[17−19]

Received: May 14, 2022
Revised: June 27, 2022
Published: July 18, 2022

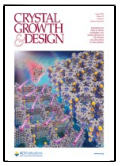

https://doi.org/10.1021/acs.cgd.2c00552
Cryst. Growth Des. 2022, 22, 5045−5053

The Scleractinia coral biomineralization process is a representative example of a heterogeneous process of nucleation and growth of $CaCO_3$.[20] Indeed, the structural formation of the skeleton starts soon after the planulae attach to a solid substrate, followed by their deposition and continued growth. However, Akiva et al. showed the presence of ACC and small aragonite crystallites in the presettled larva.[21] These precursors evolve into mature aragonitic fibers, which are characteristic of the stony coral skeleton,[22−25] by heterogeneous particle attachment processes mediated by proteins and magnesium ions.[21]

The key features of the substrates that favor coral larval adhesion and the following processes are still a theme of debate because various natural cues influence Scleractinian corals' settlement behavior.[26] The best known natural cues are the biochemical signals arising from the Mg-calcite associated with mineralized crustose coralline algae (CCA).[26,27] It has been also reported by *in vivo* observation that in the planula, aragonite forms on first-formed Mg-calcite crystals.[28]

Despite the relevance of the substrate in the different steps of the formation of the coral skeleton and the central role that Mg-calcite appears to have, few studies have investigated its role in the deposition of $CaCO_3$ *in vitro* and in the presence of the major additives, SOMs and magnesium ions. As stated above, in the subtropical scleractinians, *Stylophora pistillata* and *Pocillopora acuta*, the first mineral formed and deposited after the planula settlement was reported as Mg-calcite, whereas aragonite crystals developed between these structures and formed spherulite-like aggregates.[21,28] Njegić Džakula et al. showed by the analyses of the kinetic and thermodynamic data that in a chemical system similar to seawater, *i.e.*, having a high concentration of magnesium ions, together with low $CaCO_3$ supersaturation (Ω), the SOMs from *Balanophyllia europaea* or *Leptopsammia pruvoti* affected the aggregation of overgrowing crystalline units on aragonite seeds.[29] A calcium carbonate overgrowth experiment on coral skeletons showed the formation of aragonite crystals with a seemingly species-specific texture. In this case, magnesium ions were absent and the SOM molecules were diffused from a skeletal substrate.[30] The variation of magnesium ion concentrations in chemical systems, which mimicked the typical pH and Ω known for the calcifying fluid in corals, highlighted the inhibiting effect of magnesium ions, regardless of pH and Ω values.[24,31]

The proposed hypothesis is that Mg-calcite crystals, reported as a substrate on which the coral larvae attach to and on which the planula produce Mg-calcite to grow the aragonitic skeleton, affect the capability of SOMs and magnesium ions to influence the precipitation of $CaCO_3$. To verify this hypothesis, $CaCO_3$ overgrowth has been performed using calcite and Mg-calcite seeds in the presence of precipitating media containing SOMs and magnesium ions. The SOMs extracted from the skeletons of the Mediterranean Sea stony coral, *Oculina patagonica*, or the Indo-Pacific stony coral, *S. pistillata*, were used to represent coral species with different growth strategies and living conditions and environments.

EXPERIMENTAL SECTION

Materials. All chemicals were obtained from Merck, analytical grade, and used without further purification. All glassware was cleaned in ethanol and rinsed with distilled water before being dried in air.

Extraction of the Organic Matrix. The soluble (SOM) and the insoluble OM (IOM) fractions were extracted through decalcification using a 0.1 M CH_3COOH solution, as previously reported.[30] The skeletons of the Mediterranean Sea stony coral, *O. patagonica*, and the Indo-Pacific stony coral, *S. pistillata*, were used. The SOM concentration was expressed as the amount of protein from the amino acid analysis.

Calcium Carbonate Seed Crystal Syntheses. A 30 cm diameter desiccator was utilized for seed synthesis. It contained one glass beaker (50 mL) with crushed ammonium carbonate powder covered with parafilm, punched with three needle holes, and a Petri dish containing 5 g of anhydrous $CaCl_2$. These were placed at the bottom of the desiccator in advance. Microplates for cellular culture containing a round glass coverslip in each well were used. Each well containing 750 μL of 10 mM $CaCl_2$ solution or of 10 mM $CaCl_2$ and 10 mM $MgCl_2$ solution was prepared. After a 4-day crystallization time, the glass coverslips were lightly rinsed with Milli-Q water, dried, and examined using an optical microscope. The crystals on some coverslips, after gold coating, were examined with a scanning electron microscope.

Calcium Carbonate Overgrowth Experiments on Mg-Calcite or Calcite Crystal Seeds. The crystallization desiccator utilized for seed synthesis, containing $(NH_4)_2CO_3$ and anhydrous $CaCl_2$, was used. In each well of the microplate for cellular culture, a round coverslip having on its surface the seeds of either calcite or Mg-calcite was inserted, and 750 μL of an aqueous solution of either 10 mM $CaCl_2$ or 10 mM $CaCl_2$ and 10 mM $MgCl_2$ (Mg/Ca molar ratio equal to 1, hereafter named MgCa) was used. In these systems, the SOM from either *O. patagonica* or *S. pistillata* was used at a concentration of 13.3 or 33.3 μg/mL, respectively. These concentrations were defined after preliminary investigation in a homogeneous precipitation system (Figures SI1−SI4).[32] After a 4-day crystallization time, the glass coverslips were lightly rinsed with Milli-Q water, dried, and examined using an optical microscope.

Characterization of Calcium Carbonate Precipitates. The optical microscope observations of $CaCO_3$ precipitates were made using a Leica microscope equipped with a digital camera. The scanning electron microscopy (SEM) images were acquired using a Leica Cambridge Stereoscan 360 scanning electron microscope. The samples were gold coated (2 nm) before their observation. A Thermo Scientific Nicolet iS10 Fourier transform infrared (FTIR) spectrometer was used to collect the FTIR spectra. The disk sample for FTIR analysis was obtained by mixing a small amount (<1 mg) of the product with 100 mg of KBr and applying a pressure of 45 tons per square inch (620.5 MPa) to the mixture using a press. X-ray diffraction patterns were collected using a PANanalytical X'Pert Pro diffractometer equipped with a multiarray X'Celerator detector using Cu Kα radiation generated at 40 kV and 40 mA (λ = 1.54056 Å). The diffraction patterns were collected in the 2θ range between 20 and 60° with a step size ($\Delta 2\theta$) of 0.02° and a counting time of 100 s. The refinement of the X-ray diffraction patterns for the determination of the unit cell parameter was performed using the software Profex.[33]

Raman spectra were collected using a LabRAM HR Evolution instrument (Horiba, France). The instrument is equipped with an 800 mm spectrograph which allows for sub-two wavenumber pixel spacing when working with a 600 grooves/mm grating at the an excitation wavelength of 532 nm. The sample was exposed to the laser light by a 50× LWD NA = 0.5 objective (LMPlanFL N, Olympus, Japan). The LabRAM instrument has a 1024 × 256 pixel, open-electrode, front illuminated, cooled charge-coupled device (CCD) camera. The system is set around an open confocal microscope (BXFM Olympus, Japan) with a spatial resolution of 2 μm using a 50× objective. Exposures between 15 s and 1 min were used. This system is equipped with ultralow frequency capability, four laser lines, many objectives, and several gratings to allow modular and flexible use for samples of great variability.

RESULTS

A series of overgrowth experiments were performed using the vapor diffusion method on calcite or Mg-calcite seeds.[34] The seed crystals of calcite showed the typical {104} rhombohedral faces, while those of Mg-calcite showed additional rhombohe-

https://doi.org/10.1021/acs.cgd.2c00552
Cryst. Growth Des. 2022, 22, 5045−5053

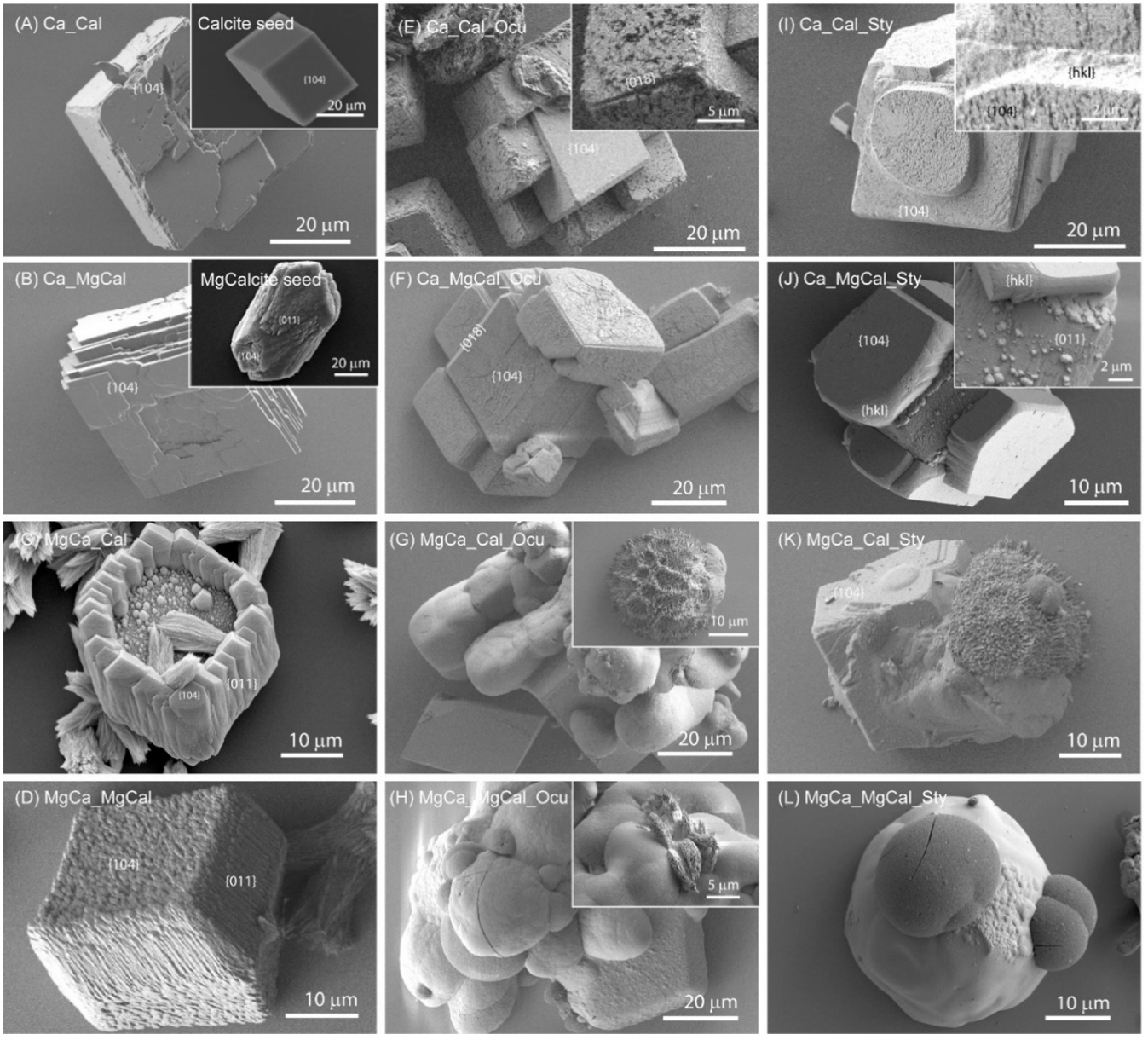

Figure 1. SEM images of calcium carbonate products obtained from overgrowth experiments. (A–D) Control experiments, *i.e.*, overgrowth experiments in the absence of SOM. (E–H) Overgrowth experiments in the presence of 13.3 μg/mL SOM extracted from *O. patagonica*. (I–L) Overgrowth experiments in the presence of 33.3 μg/mL SOM extracted from *S. pistillata*. The text of the label that follows the letter is reported for the sake of clarity. Ca and MgCa indicate 10 mM $CaCl_2$ solution and 10 mM $MgCl_2$ solution, respectively. Cal and MgCal indicate calcite seed and magnesium calcite seed, respectively. Ocu and Sty indicate the presence of SOM from *O. patagonica* and *S. pistillata*, respectively. The insets show details of the $CaCO_3$ overgrowth. The Miller indices of the crystalline faces are reported.

dral {011} faces due to the interaction of magnesium ions with the growing crystals and irregular {104} faces (Figure 1A,B; insets).[35] The surface texture of newly expressed {011} faces showed the presence of {011} steps closed by {104} faces. When Mg-calcite seeds were precipitated, the copresence of acicular crystals of aragonite was also observed. The X-ray powder diffraction patterns confirmed the morphologically assigned mineral phases (Figure SI5), and the analysis of the diffraction pattern of Mg-calcite indicated an isomorphic substitution of magnesium ions by calcium ions of about 4 atom %.[35]

Overgrowth control experiments were performed without SOM (Figure SI6). The deposition of additional calcite {104} layers on the calcite seeds was observed from the 10 mM $CaCl_2$ solution (Figure 1A); on Mg-calcite seeds of the same solution, the overgrowth of {104} calcite crystals occurred, in some cases until the complete covering of the seed crystals and the disappearance of the rhombohedral {011} faces (Figure 1B). When the overgrowth was performed from the MgCa solution on calcite crystals, the formation of crystal exposing the typical {011} faces of Mg-calcite was observed together with {104} faces (Figure 1C). The overgrown crystals displayed the same crystallographic orientation as the substrate. Interestingly, overgrowth crystals nucleated in lines, which run diagonally to the rhombohedral {104} faces of the substrate. A similar scenario was observed when the overgrowth occurred from the MgCa solution on Mg-calcite seeds (Figure 1D). In this case, the seed crystals were covered

https://doi.org/10.1021/acs.cgd.2c00552
Cryst. Growth Des. 2022, 22, 5045–5053

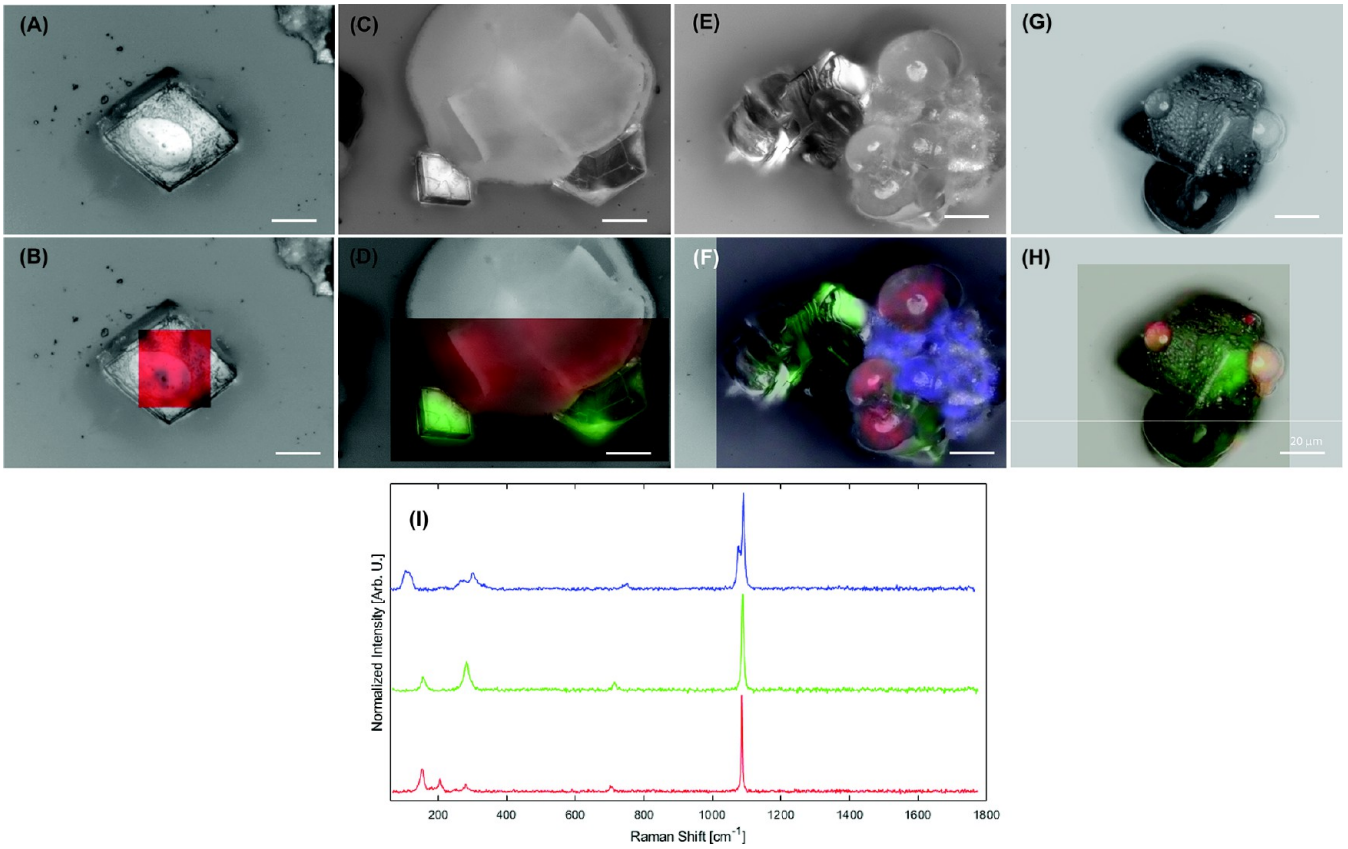

Figure 2. Raman microscope analyses on $CaCO_3$ obtained from overgrowth experiments. (A, B) Optical microscopy image and mineral phase overlaid color map, respectively, of $CaCO_3$ overgrown on a calcite seed from a 10 mM $CaCl_2$ solution in the presence of 33.3 μg/mL SOM from *S. pistillata*. (C, D) Optical microscopy image and mineral phase overlaid color map, respectively, of $CaCO_3$ overgrown on a calcite seed from a 10 mM $CaCl_2$ solution in the presence of 13.3 μg/mL SOM from *O. patagonica*. (E, F) Optical microscopy image and mineral phase overlaid color map, respectively, of $CaCO_3$ overgrown on a Mg-calcite seed from a 10 mM $CaCl_2$ and 10 mM $MgCl_2$ solution in the presence of 33.3 μg/mL SOM from *S. pistillata*. (G, H) Optical microscopy image and mineral phase overlaid color map, respectively, of $CaCO_3$ overgrown on a Mg-calcite seed from a 10 mM $CaCl_2$ and 10 mM $MgCl_2$ solution in the presence of 13.3 μg/mL SOM from *O. patagonica*. (I) Raman spectra of calcite (red), aragonite (green), and vaterite (blue) from the respective overgrowth experiments. The color maps indicate calcite (red), aragonite (green), and vaterite (blue). Scale bar: 20 μm.

entirely by {011} faces of Mg-calcite. X-ray powder diffraction analysis confirmed the morphological assignment of the mineral phase (Figure SI7).

The addition of SOM to the crystallization solution leads to similar trends in the crystal overgrowth on calcite and Mg-calcite seeds, with some specific distinctions. The obtained products were characterized, and each species produced distinctive characteristics and mineral patterns of the overgrown crystals.

In general, the formation of crystalline-like structures occurred on the seeds from the Ca solution, while from the MgCa solution, the formation of globular and spheroidal shapes was observed (Figures SI8 and SI9). On calcite seeds from the Ca solution, with *O. patagonica* SOM (indicated as Ocu in the figure), a regular form of calcite overgrew, covering some of the crystal edges (Figure 1E). In contrast, with the presence of *S. pistillata* SOM (named Spy in the figure), the formation of disk-like shapes centered on each {104} face of the calcite seed was observed (Figure 1I).

The overgrown calcite left uncovered the crystal edges and showed the surface rich in irregular pits (Figure 1I inset). The Raman spectroscopy investigation revealed that this structure was made of calcite (Figure 2I). On Mg-calcite seeds from the Ca solution, the presence of *O. patagonica* SOM provoked the deposition of calcite crystals that, as observed on calcite seeds, developed on the {104} faces (Figure 1F), covering all of the seed edges, showed {018} faces on their edges, and had pitted surfaces (Figure 1F). Meanwhile, in the presence of SOM from *S. pistillata*, the overgrown calcite did not cover the seed completely leaving the {011} faces of Mg-calcite seeds exposed (Figure 1J). Furthermore, the overgrown calcite crystals were more pitted in the presence of *O. patagonica* SOM than *S. pistillata* SOM (Figure 1F,J), but the latter induced a stronger change in the crystalline shape stabilizing the formation of {*hkl*} faces almost parallel to the crystallographic *c*-axis of calcite (Figure 1J).

As for growth on calcite seeds from the MgCa solution, spheroidal shapes with some evidence of crystalline faces covered almost completely the calcite seed in the presence of *O. patagonica* SOM (Figure 1G), and they were made of Mg-calcite, although in a few cases, the presence of vaterite was also detected (Table 1 and Figure 2F). This effect was less marked in the presence of *S. pistillata* SOM (Figure 1K), where irregular disk-like structures were present on {104} faces together with small spheroidal structures. In both cases, the formation of acicular structures was observed on the top of the spheroidal structures, and in some cases, they completely covered the seed (Figure 1G inset). The latter was made of

https://doi.org/10.1021/acs.cgd.2c00552
Cryst. Growth Des. 2022, 22, 5045−5053

Table 1. Summary of the Results Obtained from the Overgrowth Experiments in the Presence of Seeds and SOM Extracted from *O. patagonica* and *S. pistillata*[a]

coral species	solution	seeds	overgrowth phase	shape
control	Cal	Cal	C	{104}; rh.
	Cal	MgCal	C	{104}; rh. ass.
	MgCa	Cal	MgC, A[b]	{011}, {104}; rh. ass.
	MgCa	MgCal	MgC, A[b]	{011}, {104}; rh. ass.
O. patagonica	Cal	Cal	C	{018}, {104}; rh. ass. rough
	Cal	MgCal	C	{018}, {104}; rh. ass. rough
	MgCa	Cal	MgC, A, (V)[c]	spher., needle agg.
	MgCa	MgCal	A, (ACC)[d]	glob., needle agg.
S. pistillata	Ca	Cal	C, (V)[c]	disk. rough
	Ca	MgCal	C	{hkl}, {104}; rh. ass.
	MgCa	Cal	MgC, A	disk, spher. needle agg.
	MgCa	MgCal	A, (ACC)[d]	glob., needle agg.

[a]C, A, MgC, V, and ACC indicate calcite, aragonite, Mg-calcite, vaterite, and amorphous calcium carbonate, respectively. The shape of the crystals has been defined as follows: rh = rhombohedral; disk = disk-like structure; spher. = spheroidal; glob. = globular structure; and needle = needle-like structures. Ass. indicates that the overgrowth of single crystal occurred on more faces of the same seed; this was considered as an assembly of crystals. Agg. indicates aggregates of needle particles without a defined order. [b]Aragonite aggregates were observed in the proximity of calcitic seed. [c]In a few seeds, Raman spectra indicated the copresence of vaterite. [d]There is no direct evidence of the presence of ACC; the globular shapes of the particles as well as the content of water in them may suggest an initial presence as a transient form.

aragonite (Figure 2). In the presence of Mg-calcite seeds, globular shapes formed in the presence of both SOMs (Figure 1H,L). They were made of aragonite (Figure 2). We had no evidence of the presence of ACC from Raman spectra. However, it has to be considered that micro-Raman spectroscopy is not a surface technique and thus thin superficial layers of ACC could not be detected. *O. patagonica* SOM affects the overgrowth differently from *S. pistillata* SOM, the latter favoring the formation of more regular globular shapes on/from which acicular aggregates formed. These globular shapes broke under the electron beam. This can be caused by the presence of entrapped water but can also be a unique growth texture of the deposited mineral phase. Observations on intermediate stages of overgrowth suggest that independently of the crystallization system growth starts from the {104} faces of the seeds, regardless of whether they are calcite or Mg-calcite (Figure 3).

The overgrowth on aragonite seed aggregates was not investigated in the present study. This was due to the difficulty in identifying the overgrown $CaCO_3$, since aragonite does not form single crystals, as calcite and Mg-calcite do, but acicular aggregates. The general goal of this research was to investigate the overgrowth process on calcite and Mg-calcite crystal seeds.

DISCUSSION

The literature reports that the first stages of the structural coral calcification process, the adhesion to the substrate and the initial skeleton formation, can occur on substrates based on Mg-calcite, mainly from CCA,[26] and most importantly that the first mineral phase deposited in the planula is Mg-calcite and the growth of fibrous aragonite occurs on this substrate.[21,28] However, the influence of the presence of SOM macromolecules and magnesium ions on the calcification process on Mg-calcite crystal seeds has not yet been investigated by *in vitro* studies. These two additives have been shown to influence the deposition of $CaCO_3$ through many *in vitro* experiments.[21,24,28,30,36−38] The effect of magnesium ions, particularly, appears to be a distinctive feature of coral calcification. In mollusk shells, it has long been established that the SOM alone can guide the formation of aragonite in specific media, even in the absence of magnesium ions.[39−41] On the contrary, the reported *in vivo* and *in vitro* experiments suggest that stony corals can induce aragonite formation through an ACC precursor phase,[9,30] in which magnesium ions have a crucial role.[21,24,28,30,36−38] Moreover, a converging set of experimental data in homogeneous systems shows that the presence of SOM in solution favors the formation of Mg-calcite instead of aragonite, regardless of the investigated species.[42,43] This has also been shown using the specific coral acidic recombinant proteins, CARP3, in *in vitro* experiments.[44] Moreover, CARP3 induces aragonite formation in seawater and stabilizes the formation of a thin layer of vaterite when preadsorbed on calcite crystals in the absence of magnesium ions.[45]

The results of the overgrowth experiments are in line with the previous literature, highlighting the critical role of magnesium ions and SOMs. When only SOM was present in the solution, the $CaCO_3$ overgrowth on calcite and Mg-calcite altered with the SOM source. The presence of SOM from *O. patagonica* did not change the shape features of the overgrown calcite on the calcite seed, having an apparent epitaxial growth of crystalline blocks surrounding the seed edges and conserving the {104} faces,[46,47] although these faces showed a more irregular surface ascribable to the adsorption of SOM molecules.[32,48,49] These observations were also maintained when the overgrowth occurred on Mg-calcite seeds, which is different from the control, which is SOM free. This overgrowth mechanism seems to be a feature of the SOM from *O. patagonica*, irrespective of the different seed crystals used. Conversely, the SOM from *S. pistillata* favored an overgrowth mechanism in which the epitaxy occurred on the {104} faces, independently from the seed crystal of calcite or Mg-calcite. In this case, the overgrowth calcite showed a different shape and morphology from the control. These observations suggest a diverse capability of the two SOMs to interact with the seed and the growing $CaCO_3$, which could be related to their different amino acid compositions and proteins.[32] It is known that there is an increase in SOM molecule concentrations near the surface that changes the activity of the solution close to the crystal face, leading to a decrease in surface energy, which in turn reduces the nucleation barrier favoring the overgrowth.[50,51] This peculiar condition could favor the formation of a liquid-phase mineral precursor, as observed for the formation of calcite fibers on existing calcite substrate crystals.[52]

In the presence of magnesium ions in the solution, the overgrowth of polycrystalline Mg-calcite crystals was observed. This overgrowth differs in the crystal shape and morphology and the coverage of the seed crystals according to the used seed. The Mg-calcite overgrown on Mg-calcite seeds exposes more {011} faces and covers the seed crystals completely compared to that on calcite seeds. We can suppose that the {011} faces act as a favorable template for the growth of Mg-calcite. This peculiar controlled assembly of Mg-calcite crystals has not been reported so far in the literature.

https://doi.org/10.1021/acs.cgd.2c00552
Cryst. Growth Des. 2022, 22, 5045−5053

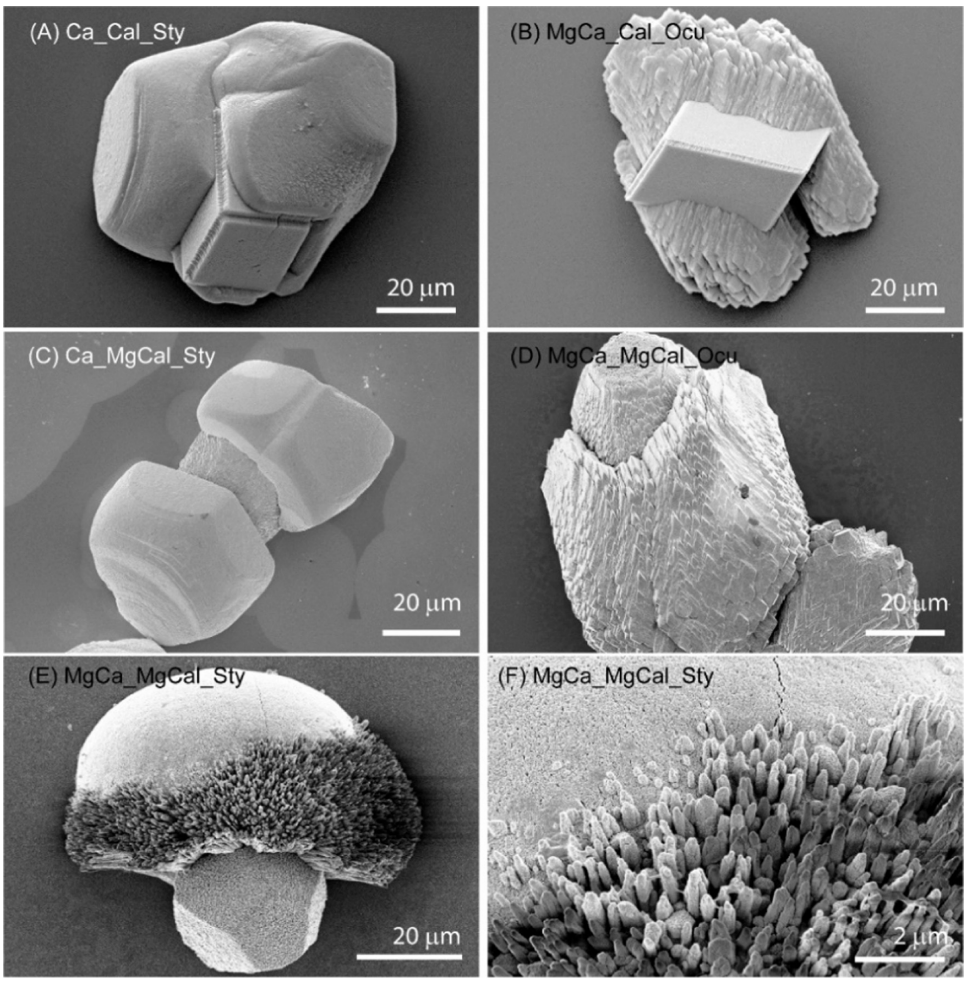

Figure 3. SEM images of calcium carbonate overgrowth experiments at different stages of growth of some representative experiments. (A, C, E, F) Overgrowth experiments in the presence of 33.3 μg/mL SOM extracted from *S. pistillata*. (B, D) Overgrowth experiments in the presence of 13.3 μg/mL of SOM extracted from *O. patagonica*. The label that follows is reported for clarity. Ca and MgCa indicate 10 mM $CaCl_2$ solution and 10 mM $CaCl_2$ and 10 mM $MgCl_2$ solution, respectively. Cal and MgCal indicate calcite seed and magnesium calcite seed, respectively. Ocu and Sty indicate the presence of SOM from *O. patagonica* and *S. pistillata*, respectively.

The copresence in the solution of SOMs and magnesium ions reduced the different capabilities of the two SOMs in affecting the overgrowth of $CaCO_3$. Spheroidal shapes of aragonite (Raman data, Figure 2) from which acicular crystals emerged were always observed, independently of the seed and the SOM used. These spheroids were more elongated when using the SOM from *O. patagonica* than from *S. pistillata*. This difference is more evident with calcite seeds than with the Mg-calcite ones. On the former, the SOM from *S. pistillata* also induces calcification effects resembling those observed in the absence of magnesium ions. Remarkably, the differences of the SOMs in affecting the overgrowth of $CaCO_3$ are no longer noticeably evident when Mg-calcite seeds are used.

The spheroidal shapes are formed by aragonite, and their shape could be the evidence of a transient amorphous phase, which, however, was not observed. The stabilization of magnesium ions and SOMs of ACC has been previously reported.[9,30] In the ammonium carbonate vapor diffusion method precipitation system used in this research, the mineral phase is analyzed after a reaction time of 4 days.[34] It cannot be excluded that ACC crystallizes in this reaction time, even if an ACC stabilization from the organic matrix macromolecules has been reported for other *in vivo* calcium carbonate precipitation systems.[30] In an *in vivo* experiment, it was shown that ACC and aragonite coexist even before the planula attachment.[9] In *in vitro* experiments, the formation of ACC submicron particles that converted to Mg-calcite upon heating was observed, except when the SOM from *B. europaea* was present and aragonite coformed.[30] Here, we observed that the aragonite overgrown on Mg-calcite appeared as needles coexisting with spheroidal shapes (Figure 3). This could involve a mechanism of phase microstructural reorganization associated with nanoparticle reassembly, as already observed for calcite in a hydrogel[53] and in the presence of synthetic polyelectrolytes.[54,55] In a previous study, the overgrowth of aragonite, as prisms, was observed only on the aragonitic coral skeleton and was described as a secondary nucleation event.[30] Here, the mechanism of aragonite formation, besides the cited phase microstructural reorganization, has to take into account the Mg-calcite substrate. The SOM molecules adsorb on the crystal face, leading to a decrease in surface energy[51] and favoring the heterogeneous nucleation process.[56] However, this consideration alone does not explain the preferential formation of aragonite on Mg-calcite seeds with respect to calcite seeds in the presence of SOMs and magnesium ions. Thus, we can speculate that the SOM molecules when adsorbed on the Mg-

https://doi.org/10.1021/acs.cgd.2c00552
Cryst. Growth Des. 2022, 22, 5045−5053

calcite crystals, their natural substrate *in vivo*, act as a template for the nucleation of aragonite or favor the phase transition to aragonite from an ACC precursor. Such a speculation is in line with one of the pioneering paradigms of biomineralization: biomineralizing macromolecules are able to perform their action as controllers of mineral phase polymorphism only when adsorbed on specific substrates.[39,41,57]

CONCLUSIONS

In conclusion, this study showed that SOMs from *S. pistillata* and *O. patagonica* have different effects on the overgrowth of $CaCO_3$ on Mg-calcite and calcite seeds, but these differences are less evident in the presence of magnesium ions. Moreover, the Mg-calcite is a favorable substrate for the overgrowth of aragonite, differently from calcite. This may occur through an ACC transient phase in agreement with data reported in *in vivo* experiments and a template effect of the adsorbed SOM molecules. The overall results of this study highlight the importance of magnesium ions in defining the shape, morphology, and polymorphism of bioproduced $CaCO_3$. They also suggest a magnesium-dependent biological control on the deposition of the coral skeleton.

ASSOCIATED CONTENT

Supporting Information

The Supporting Information is available free of charge at https://pubs.acs.org/doi/10.1021/acs.cgd.2c00552.

Detailed description of the experimental section, selection of the optimal SOM concentration for $CaCO_3$ overgrowth experiments, additional optical and scanning electron microscopy images, and FTIR spectra and X-ray diffraction patterns (PDF)

AUTHOR INFORMATION

Corresponding Authors

Tali Mass − *Department of Marine Biology, The Leon H. Charney School of Marine Sciences, University of Haifa, 3498838 Haifa, Israel*; Email: tmass@univ.haifa.ac.il

Giuseppe Falini − *Department of Chemistry 'Giacomo Ciamician', University of Bologna, 40126 Bologna, Italy; Institute for Nanostructured Materials, CNR, 40129 Bologna, Italy*; orcid.org/0000-0002-2367-3721; Email: giuseppe.falini@unibo.it

Authors

Tal Zaquin − *Department of Marine Biology, The Leon H. Charney School of Marine Sciences, University of Haifa, 3498838 Haifa, Israel*

Iddo Pinkas − *Department of Chemical Research Support, Weizmann Institute of Science, 76100 Rehovot, Israel*; orcid.org/0000-0001-7434-9844

Anna Paola Di Bisceglie − *Department of Chemistry 'Giacomo Ciamician', University of Bologna, 40126 Bologna, Italy*

Angelica Mucaria − *Department of Chemistry 'Giacomo Ciamician', University of Bologna, 40126 Bologna, Italy*

Silvia Milita − *CNR—Institute for Microelectronic and Microsystems, 40129 Bologna, Italy*; orcid.org/0000-0002-9612-2541

Simona Fermani − *Department of Chemistry 'Giacomo Ciamician', University of Bologna, 40126 Bologna, Italy*

Stefano Goffredo − *Marine Science Group, Department of Biological, Geological and Environmental Sciences, University of Bologna, 40126 Bologna, Italy; Fano Marine Center, 61032 Fano, Italy*

Complete contact information is available at: https://pubs.acs.org/10.1021/acs.cgd.2c00552

Author Contributions

The manuscript was written through contributions of all authors. All authors have given approval to the final version of the manuscript.

Funding

This research was supported by the Ministry of Innovation, Science & Technology, Israel.

Notes

The authors declare no competing financial interest.

ACKNOWLEDGMENTS

I.P. is the incumbent of the Sharon Zuckerman research fellow chair.

REFERENCES

(1) Lowenstam, H. A.; Weiner, S. *On Biomineralization*; Oxford University Press, 1989.

(2) Addadi, L.; Weiner, S. Biomineralization: Mineral Formation by Organisms. *Phys. Scr.* **2014**, *89*, No. 098003.

(3) Gadd, G. M. Fungal Biomineralization. *Curr. Biol.* **2021**, *31*, R1557−R1563.

(4) Veis, A.; Dorvee, J. R. Biomineralization Mechanisms: A New Paradigm for Crystal Nucleation in Organic Matrices. *Calcif. Tissue Int.* **2013**, *93*, 307−315.

(5) Shtukenberg, A. G.; Ward, M. D.; Kahr, B. Crystal Growth with Macromolecular Additives. *Chem. Rev.* **2017**, *117*, 14042−14090.

(6) Beniash, E.; Aizenberg, J.; Addadi, L.; Weiner, S. Amorphous Calcium Carbonate Transforms into Calcite during Sea Urchin Larval Spicule Growth. *Proc. R. Soc. London, Ser. B* **1997**, *264*, 461−465.

(7) Gilbert, P. U. P. A.; Bergmann, K. D.; Boekelheide, N.; Tambutté, S.; Mass, T.; Marin, F.; Adkins, J. F.; Erez, J.; Gilbert, B.; Knutson, V.; et al. Biomineralization: Integrating Mechanism and Evolutionary History. *Sci. Adv.* **2022**, *8*, No. eabl9653.

(8) Gilbert, P. U. P. A.; Porter, S. M.; Sun, C.-Y.; Xiao, S.; Gibson, B. M.; Shenkar, N.; Knoll, A. H. Biomineralization by Particle Attachment in Early Animals. *Proc. Natl. Acad. Sci. U.S.A.* **2019**, *116*, 17659−17665.

(9) Mass, T.; Giuffre, A. J.; Sun, C.-Y.; Stifler, C. A.; Frazier, M. J.; Neder, M.; Tamura, N.; Stan, C. V.; Marcus, M. A.; Gilbert, P. U. P. A. Amorphous Calcium Carbonate Particles Form Coral Skeletons. *Proc. Natl. Acad. Sci. U.S.A.* **2017**, *114*, E7670−E7678.

(10) Von Euw, S.; Zhang, Q.; Manichev, V.; Murali, N.; Gross, J.; Feldman, L. C.; Gustafsson, T.; Flach, C.; Mendelsohn, R.; Falkowski, P. G. Biological Control of Aragonite Formation in Stony Corals. *Science* **2017**, *356*, 933−938.

(11) Weiss, I. M.; Tuross, N.; Addadi, L. I. A.; Weiner, S. Mollusc Larval Shell Formation: Amorphous Calcium Carbonate Is a Precursor Phase for Aragonite. *J. Exp. Zool.* **2002**, *293*, 478−491.

(12) Politi, Y.; Arad, T.; Klein, E.; Weiner, S.; Addadi, L. Sea Urchin Spine Calcite Forms via a Transient Amorphous Calcium Carbonate Phase. *Science* **2004**, *306*, 1161−1164.

(13) Boon, M.; Rickard, W. D. A.; Rohl, A. L.; Jones, F. Stabilization of Aragonite: Role of Mg2+ and Other Impurity Ions. *Cryst. Growth Des.* **2020**, *20*, 5006−5017.

(14) Purgstaller, B.; Konrad, F.; Dietzel, M.; Immenhauser, A.; Mavromatis, V. Control of Mg2+/Ca2+ Activity Ratio on the Formation of Crystalline Carbonate Minerals via an Amorphous Precursor. *Cryst. Growth Des.* **2017**, *17*, 1069−1078.

(15) Wang, D.; Wallace, A. F.; De Yoreo, J. J.; Dove, P. M. Carboxylated Molecules Regulate Magnesium Content of Amorphous Calcium Carbonates during Calcification. *Proc. Natl. Acad. Sci. U.S.A.* **2009**, *106*, 21511−21516.
(16) Gower, L. B. Biomimetic Model Systems for Investigating the Amorphous Precursor Pathway and Its Role in Biomineralization. *Chem. Rev.* **2008**, *108*, 4551−4627.
(17) Raz, S.; Hamilton, P. C.; Wilt, F. H.; Weiner, S.; Addadi, L. The Transient Phase of Amorphous Calcium Carbonate in Sea Urchin Larval Spicules: The Involvement of Proteins and Magnesium Ions in Its Formation and Stabilization. *Adv. Funct. Mater.* **2003**, *13*, 480−486.
(18) Goffredo, S.; Vergni, P.; Reggi, M.; Caroselli, E.; Sparla, F.; Levy, O.; Dubinsky, Z.; Falini, G. The Skeletal Organic Matrix from Mediterranean Coral *Balanophyllia europaea* Influences Calcium Carbonate Precipitation. *PLoS One* **2011**, *6*, No. e22338.
(19) Bentov, S.; Erez, J. Impact of Biomineralization Processes on the Mg Content of Foraminiferal Shells: A Biological Perspective. *Geochem., Geophys., Geosyst.* **2006**, *7*, 1525−1536.
(20) Tambutté, S.; Holcomb, M.; Ferrier-Pagès, C.; Reynaud, S.; Tambutté, É.; Zoccola, D.; Allemand, D. Coral Biomineralization: From the Gene to the Environment. *J. Exp. Mar. Biol. Ecol.* **2011**, *408*, 58−78.
(21) Akiva, A.; Neder, M.; Kahil, K.; Gavriel, R.; Pinkas, I.; Goobes, G.; Mass, T. Minerals in the Pre-Settled Coral *Stylophora pistillata* Crystallize via Protein and Ion Changes. *Nat. Commun.* **2018**, *9*, No. 1880.
(22) Cohen, A. L.; McConnaughey, T. A. Geochemical Perspectives on Coral Mineralization. *Rev. Mineral. Geochem.* **2003**, *54*, 151−187.
(23) Cuif, J. P.; Dauphin, Y. The Environment Recording Unit in Coral Skeletons−a Synthesis of Structural and Chemical Evidences for a Biochemically Driven, Stepping-Growth Process in Fibres. *Biogeosciences* **2005**, *2*, 61−73.
(24) Comeau, S.; Tambutté, E.; Carpenter, R. C.; Edmunds, P. J.; Evensen, N. R.; Allemand, D.; Ferrier-Pagès, C.; Tambutté, S.; Venn, A. A. Coral Calcifying Fluid PH Is Modulated by Seawater Carbonate Chemistry Not Solely Seawater PH. *Proc. R. Soc. B* **2017**, *284*, No. 20161669.
(25) Drake, J. L.; Mass, T.; Stolarski, J.; Von Euw, S.; van de Schootbrugge, B.; Falkowski, P. G. How Corals Made Rocks through the Ages. *Global Change Biol.* **2020**, *26*, 31−53.
(26) Levenstein, M. A.; Marhaver, K. L.; Quinlan, Z. A.; Tholen, H. M.; Tichy, L.; Yus, J.; Lightcap, I.; Kelly, L. W.; Juarez, G.; Vermeij, M. J. A. Engineered Substrates Reveal Species-Specific Inorganic Cues for Coral Larval Settlement. *ACS Sustainable Chem. Eng.* **2022**, *10*, 3960−3971.
(27) Bianco-Stein, N.; Polishchuk, I.; Seiden, G.; Villanova, J.; Rack, A.; Zaslansky, P.; Pokroy, B. Helical Microstructures of the Mineralized Coralline Red Algae Determine Their Mechanical Properties. *Adv. Sci.* **2020**, *7*, No. 2000108.
(28) Neder, M.; Laissue, P. P.; Akiva, A.; Akkaynak, D.; Albéric, M.; Spaeker, O.; Politi, Y.; Pinkas, I.; Mass, T. Mineral Formation in the Primary Polyps of Pocilloporoid Corals. *Acta Biomater.* **2019**, *96*, 631−645.
(29) Njegić Džakula, B.; Fermani, S.; Dubinsky, Z.; Goffredo, S.; Falini, G.; Kralj, D. In Vitro Coral Biomineralization under Relevant Aragonite Supersaturation Conditions. *Chem.—Eur. J.* **2019**, *25*, 10616−10624.
(30) Reggi, M.; Fermani, S.; Landi, V.; Sparla, F.; Caroselli, E.; Gizzi, F.; Dubinsky, Z.; Levy, O.; Cuif, J.-P.; Dauphin, Y.; et al. Biomineralization in Mediterranean Corals: The Role of the Intraskeletal Organic Matrix. *Cryst. Growth Des.* **2014**, *14*, 4310−4320.
(31) Reymond, C. E.; Hohn, S. An Experimental Approach to Assessing the Roles of Magnesium, Calcium, and Carbonate Ratios in Marine Carbonates. *Oceans*; Multidisciplinary Digital Publishing Institute, 2021; Vol. 2, pp 193−214.
(32) Zaquin, T.; Di Bisceglie, A. P.; Pinkas, I.; Falini, G.; Mass, T. Similar Skeletal Properties yet Different Components - A Comparison between Distinct Stony Corals. *Sci. Rep.*, submitted for Publication, **2022**.
(33) Doebelin, N.; Kleeberg, R. Profex: A Graphical User Interface for the Rietveld Refinement Program BGMN. *J. Appl. Crystallogr.* **2015**, *48*, 1573−1580.
(34) Ihli, J.; Bots, P.; Kulak, A.; Benning, L. G.; Meldrum, F. C. Elucidating Mechanisms of Diffusion-Based Calcium Carbonate Synthesis Leads to Controlled Mesocrystal Formation. *Adv. Funct. Mater.* **2013**, *23*, 1965−1973.
(35) Falini, G.; Fermani, S.; Gazzano, M.; Ripamonti, A. Structure and Morphology of Synthetic Magnesium Calcite. *J. Mater. Chem.* **1998**, *8*, 1061−1065.
(36) Falini, G.; Reggi, M.; Fermani, S.; Sparla, F.; Goffredo, S.; Dubinsky, Z.; Levi, O.; Dauphin, Y.; Cuif, J. P. Control of Aragonite Deposition in Colonial Corals by Intra-Skeletal Macromolecules. *J. Struct. Biol.* **2013**, *183*, 226−238.
(37) DeCarlo, T. M.; Ren, H.; Farfan, G. A. The Origin and Role of Organic Matrix in Coral Calcification: Insights From Comparing Coral Skeleton and Abiogenic Aragonite. *Front. Mar. Sci.* **2018**, *5*, No. 170.
(38) Farfan, G. A.; Cordes, E. E.; Waller, R. G.; DeCarlo, T. M.; Hansel, C. M. Mineralogy of Deep-Sea Coral Aragonites as a Function of Aragonite Saturation State. *Front. Mar. Sci.* **2018**, *5*, No. 473.
(39) Falini, G.; Albeck, S.; Weiner, S.; Addadi, L. Control of Aragonite or Calcite Polymorphism by Mollusk Shell Macromolecules. *Science* **1996**, *271*, 67−69.
(40) Takeuchi, T.; Sarashina, I.; Iijima, M.; Endo, K. In Vitro Regulation of CaCO3 Crystal Polymorphism by the Highly Acidic Molluscan Shell Protein Aspein. *FEBS Lett.* **2008**, *582*, 591−596.
(41) Belcher, A. M.; Wu, X. H.; Christensen, R. J.; Hansma, P. K.; Stucky, G. D.; Morse, D. E. Control of Crystal Phase Switching and Orientation by Soluble Mollusc-Shell Proteins. *Nature* **1996**, *381*, 56−58.
(42) Falini, G.; Fermani, S.; Goffredo, S. Coral Biomineralization: A Focus on Intra-Skeletal Organic Matrix and Calcification. *Seminars in Cell & Developmental Biology*; Elsevier, 2015; Vol. *46*, pp 17−26.
(43) Pan, C.; Fang, D.; Xu, G.; Liang, J.; Zhang, G.; Wang, H.; Xie, L.; Zhang, R. A Novel Acidic Matrix Protein, PfN44, Stabilizes Magnesium Calcite to Inhibit the Crystallization of Aragonite. *J. Biol. Chem.* **2014**, *289*, 2776−2787.
(44) Gavriel, R.; Nadav-Tsubery, M.; Glick, Y.; Yarmolenko, A.; Kofman, R.; Keinan-Adamsky, K.; Berman, A.; Mass, T.; Goobes, G. The Coral Protein CARP3 Acts from a Disordered Mineral Surface Film to Divert Aragonite Crystallization in Favor of Mg-Calcite. *Adv. Funct. Mater.* **2018**, *28*, No. 1707321.
(45) Laipnik, R.; Bissi, V.; Sun, C.-Y.; Falini, G.; Gilbert, P. U. P. A.; Mass, T. Coral Acid Rich Protein Selects Vaterite Polymorph in Vitro. *J. Struct. Biol.* **2020**, *209*, No. 107431.
(46) Pimentel, C.; Pina, C. M.; Gnecco, E. Epitaxial Growth of Calcite Crystals on Dolomite and Kutnahorite (104) Surfaces. *Cryst. Growth Des.* **2013**, *13*, 2557−2563.
(47) Green, D. C.; Darkins, R.; Marzec, B.; Holden, M. A.; Ford, I. J.; Botchway, S. W.; Kahr, B.; Duffy, D. M.; Meldrum, F. C. Dichroic Calcite Reveals the Pathway from Additive Binding to Occlusion. *Cryst. Growth Des.* **2021**, *21*, 3746−3755.
(48) Meldrum, F. C. Calcium Carbonate in Biomineralisation and Biomimetic Chemistry. *Int. Mater. Rev.* **2003**, *48*, 187−224.
(49) Ihli, J.; Clark, J. N.; Kanwal, N.; Kim, Y.-Y.; Holden, M. A.; Harder, R. J.; Tang, C. C.; Ashbrook, S. E.; Robinson, I. K.; Meldrum, F. C. Visualization of the Effect of Additives on the Nanostructures of Individual Bio-Inspired Calcite Crystals. *Chem. Sci.* **2019**, *10*, 1176−1185.
(50) Hernández-Hernández, A.; Rodríguez-Navarro, A. B.; Gómez-Morales, J.; Jiménez-López, C.; Nys, Y.; García-Ruiz, J. M. Influence of Model Globular Proteins with Different Isoelectric Points on the Precipitation of Calcium Carbonate. *Cryst. Growth Des.* **2008**, *8*, 1495−1502.
(51) Jimenez-Lopez, C.; Rodriguez-Navarro, A.; Dominguez-Vera, J. M.; Garcia-Ruiz, J. M. Influence of Lysozyme on the Precipitation of

https://doi.org/10.1021/acs.cgd.2c00552
Cryst. Growth Des. 2022, 22, 5045−5053

Calcium Carbonate: A Kinetic and Morphologic Study. *Geochim. Cosmochim. Acta* **2003**, *67*, 1667−1676.
(52) Olszta, M. J.; Gajjeraman, S.; Kaufman, M.; Gower, L. B. Nanofibrous Calcite Synthesized via a Solution−Precursor−Solid Mechanism. *Chem. Mater.* **2004**, *16*, 2355−2362.
(53) Gal, A.; Habraken, W.; Gur, D.; Fratzl, P.; Weiner, S.; Addadi, L. Calcite Crystal Growth by a Solid-state Transformation of Stabilized Amorphous Calcium Carbonate Nanospheres in a Hydrogel. *Angew. Chem., Int. Ed.* **2013**, *52*, 4867−4870.
(54) Xu, A.-W.; Antonietti, M.; Yu, S.-H.; Cölfen, H. Polymer-Mediated Mineralization and Self-Similar Mesoscale-Organized Calcium Carbonate with Unusual Superstructures. *Adv. Mater.* **2008**, *20*, 1333−1338.
(55) Song, R.-Q.; Cölfen, H.; Xu, A.-W.; Hartmann, J.; Antonietti, M. Polyelectrolyte-Directed Nanoparticle Aggregation: Systematic Morphogenesis of Calcium Carbonate by Nonclassical Crystallization. *ACS Nano* **2009**, *3*, 1966−1978.
(56) Gómez-Morales, J.; Falini, G.; García-Ruiz, J. M. Biological Crystallization. *Handbook of Crystal Growth*; Elsevier, 2015; pp 873−913.
(57) Addadi, L.; Moradian, J.; Shay, E.; Maroudas, N. G.; Weiner, S. A Chemical Model for the Cooperation of Sulfates and Carboxylates in Calcite Crystal Nucleation: Relevance to Biomineralization. *Proc. Natl. Acad. Sci. U.S.A.* **1987**, *84*, 2732−2736.

https://doi.org/10.1021/acs.cgd.2c00552
Cryst. Growth Des. 2022, 22, 5045−5053